PAPER REF: 4024

STAMPING OF ADVANCED HIGH STRENGTH STEEL: comparative study of steels FE E340, FE 600DP and FE 800DP

Gilmar Cordeiro da Silva[1(*)], Henrique da Cruz Amaral[1(*)], José Rubens Gonçalves Carneiro[1(*)],Tarcísio José de Almeida[1(*)]

[1]Polytechnic Institute of PUC-Minas (IPUC), Pontifical Catholic University of Minas Gerais, Belo Horizonte, Brazil

[(*)]*Email:* gilmarcord@gmail.com, c.amaralhenrique@gmail.com, joserub@pucminas.br, brasiaco@superig.com.br

ABSTRACT

Currently, the automotive industry has used more complex forms in the design of their vehicles. The manufacturing of metal components that compose the body structure of a vehicle has originated from process of mechanical forming of sheet metal. The stamping was well diffused for forming process in the automotive industry. Through this process, products are obtained with the desired shape and / or required by the manufacturer. The auto industry, in order to obtain weight reduction of vehicles and also to increase the strength of their bodies, has promoted great advances in the evolution of metallurgy steels, using lightweight steels and of high mechanical strength.

This work analyzes the mechanical characteristics and the forming ability of high strength steels, used for building bodies for passenger vehicles. Three types of materials were analyzed: FE E340, FE 600DP and FE 800DP, all can be used for stamping of B-pillar reinforcement, this part is responsible for uniting the side rails and roof, as well as reducing the lateral intrusion in a collision with another vehicle. Primarily, it was necessary to investigate the basic characteristics of the materials selected. Through chemical analysis, it was possible to identify if the materials were in accordance with their specifications. The metallographic analysis provided information about the metallurgy of these materials. The microhardness testing and the tensile testing showed the mechanical strength which these materials could offer. The forming limit diagram was important to determine which of the steels studied were able to combine better structural strength, required for the B-pillar reinforcement, and the good forming ability.

Keywords: microstructure, mechanical characteristics, stampability, forming limit diagram (FLD).

INTRODUCTION

It is impossible at the development stage of modern society, to imagine the world without the use of steel. The steel production is a strong indicator of the stages of development of a country. The steels are present in daily life, but to manufacture them or use them, require necessary techniques that should be renewed cyclically.

Due to fuel efficiency, emissions reductions, and vehicle safety requirements, the auto industry has used steels that combine high strength and lightweight in their auto bodies (CORA ÖMER Necati; Muammer KOÇ, 2009). Because of the new steels, the stampability is very important and a recurring theme during the steel selection process, with these features, to be used in an auto body.

The advanced high-strength steels (AHSS) are defined as multi-phase steels consisting of ferrite, bainite, restrained austenite, and martensite. The DP steel is produced by inter-critical heat treatment, which involves quenching from a suitable temperature AC1 and AC3 (WANG WU-RONG; HE CHANG-WEI; ZHAO ZHONG-HUA; WEI XI-CHENG, 2011). The FE E340 has elements of low alloy to help its stampability. The DP steels consist of a ferritic matrix containing a hard martensitic second phase. Increasing the volume fraction of hard second phase generally increases the strength. (WORLD AUTOSTEEL, 2009)

A forming limit diagram (FLD) is a graph that shows the behavior of sheet metal under different levels of strain (from stretching to deep drawing). A forming limit diagram provides information on the maximum stress the sheet metal could undergo before fracturing or necking. This concept was introduced by Keeler and Goodwin and has been used widely as one of the criteria for optimizing a stamping process (WOLFGANG BLECK; ZHI DENG; KOSTAS PAPAMANTELLOS; CHRISTOPHER OLIVER GUSEK, 1997).

In this work, an analysis about the basic features of three high strength materials was carried out and an experimental forming limit diagram was drawn based on the Nakazima test method. These tests and analysis allowed for the comparison of the main characteristics of studied steels as well as its applications in the automotive industry.

EXPERIMENTAL PROCEDURE

The Figure 1 shows the procedure used to execute all process, from materials selection to conclusions at end of study.

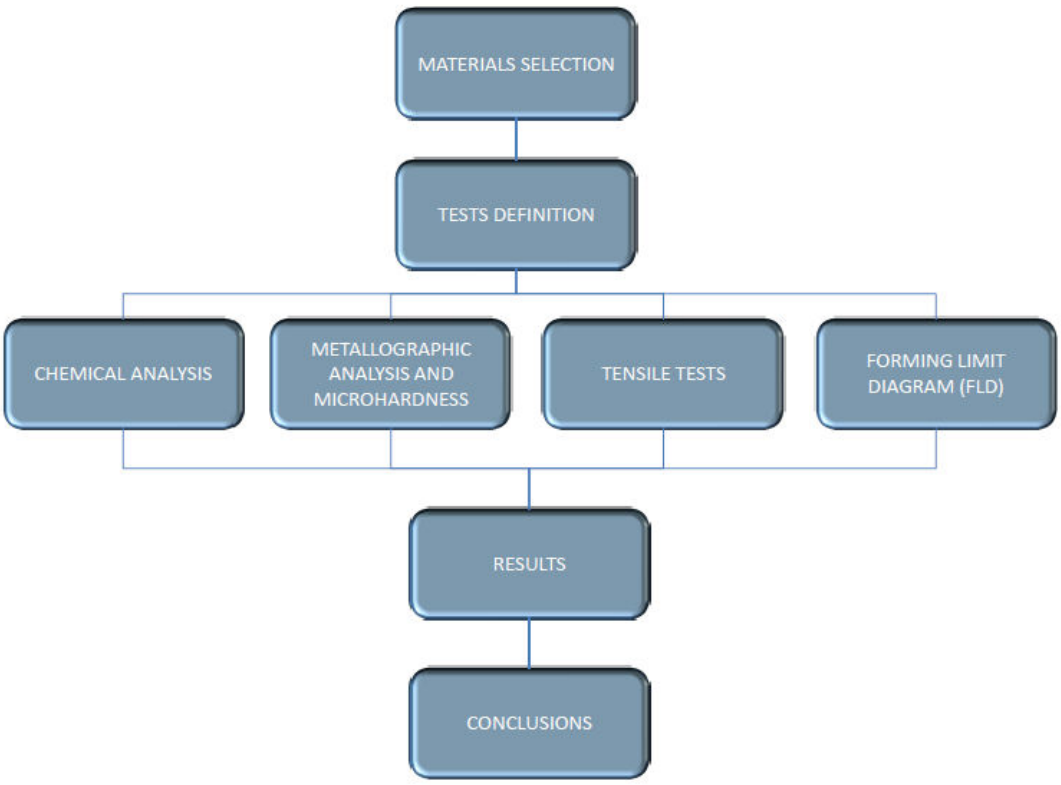

Figure 1 – Tests and analysis methodology.

Materials Selection

The materials selection took into account the possibility to compare different materials and its applications in the auto industry. A search was performed among the pieces used to build the automotive bodies; they should have had a similar applicability and different mechanical proprieties. The component selected was the B-pillar reinforcement, as shown in Figure 2, it must have good stampability and simultaneously adequate structural strength to connect the side members of the vehicle and the roof, while reduce the intrusion during a lateral crash against another vehicle. The high strength materials chosen with these characteristics were the FE E340, FE 600DP and the FE 800DP.

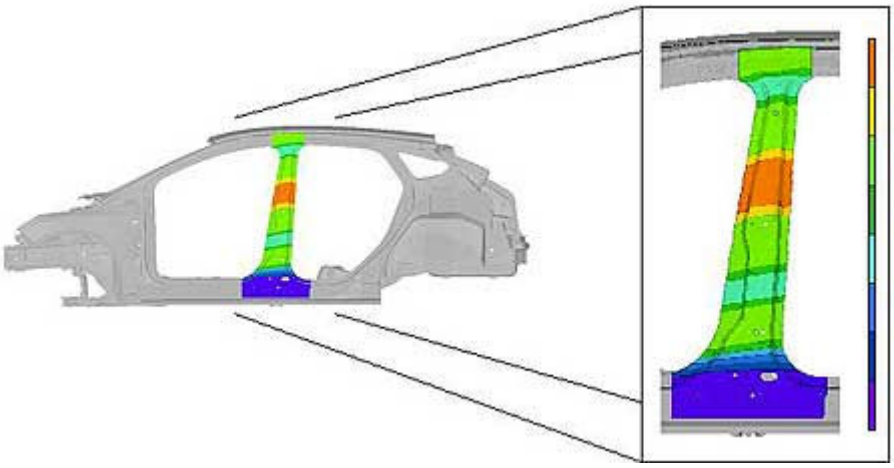

Figure 2 – Schematic B-pillar reinforcement.

The steel sheet from which samples were collected for testing had the following characteristics:

FE E340 – Cold rolled – Initial dimension (1440x530) mm, thickness of 1,2 mm.

FE 600DP – Cold rolled – Initial dimension (1450x980) mm, thickness of 1,2 mm.

FE 800DP – Cold rolled – Initial dimension (1285x400) mm. Thickness of 1,0 mm.

Chemical Analysis

The samples for chemical analysis were cut, in a dimension of (20x20) mm, in a cutting machine Struers Discotom-2. The chemical analysis was done in spectrometer of optical emission ARL Metals Analyser.

Metallographic Analysis

The samples for metallographic analysis were cut in transversal and longitudinal positions regarding direction of lamination, in a dimension of (10x30) mm, in a cutting machine Struers Discotom-2. Then, they were embedded hot in a machine Struers Prontopress-20; plastic resin was used for the embedding process. The nominal pressure used was 150 kgf/mm^2, the heating time was 8 minutes and the cooling time was 4 minutes.

The samples were sanded in grit sizes 180, 220, 320, 400, 600, 1200 and 2000 mesh, and then polished in a Naplan paper using Alumina in suspension in grit size 1 μm and distilled water for lubrification. The samples were attacked in a solution of Nital 10% and analyzed in a optical microscope.

Microhardness Testing

The test of micro-hardness Vickers was done using a diamond indenter in pyramidal format and load of 10 kgf. The test time was 15 seconds and the temperature was 22°C. The equation 1 was used to determine the Vickers micro-hardness.

$$HV = 1{,}854 \times \frac{P}{d^2} \quad (1)$$

Where:

P = load [kgf]

d = average diagonal [m]

A test was done using the embedding samples, being 10 samples for longitudinal measurements and 10 samples for transversal measurements, in total 60 measurements regarding the three materials.

Tensile Testing

The tensile specimen was obtained through forming process of shearing using a standard die cutting. The standard dimensions of specimen are showing in a schematic Figure 3.

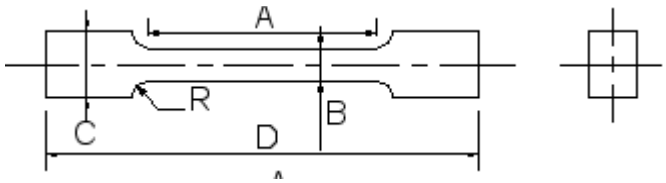

Figure 3 – Schematic standard specimen

Where:

A = 80 mm;

B = 20 mm;

C = 40 mm;

D = 255 mm;

R = 20 mm;

The specimens were sanded along its working length (A). This process is intended to reduce stress points due the shearing process made earlier. The tensile test was done based on the European Standard ISO EN 10002-1 from July 2001.

The test was carried out in universal test machine made by Instron with a nominal capacity of 50 kN. The velocity used during the testing was 1,2 cm/min for elastic regime and 34 cm/min for plastic regime. The temperature was 24°C, being tested 5 specimens for longitudinal direction of lamination and 5 specimens for transversal direction of lamination. The value of the yield strength was obtained from the stress-strain graph from the deformation of 0.2%. An optical extensometer was used to measure the longitudinal and transversal deformations along the length and width respectively.

The yield strength was calculated using Equation 2.

$$\sigma = \frac{F}{A_0} \tag{2}$$

Where:

σ = Conventional stress.

F = Force

A_0 = Initial Area

The value of the maximum load was reached in the peak load curve due to the variation of the initial length. Stretching was calculated by Equation 3.

$$\mathrm{e} = \frac{l - l_0}{l_0} = \frac{\Delta l}{l_0} \tag{3}$$

Where:

e = Conventional strain.

l = Final length.

l_0 = Initial length.

The true strain and true stress are given by the Equations 4 and 5:

$$\varepsilon = \ln(1 + \mathrm{e}) \tag{4}$$

$$\sigma_r = \sigma(1 + \mathrm{e}) \tag{5}$$

Where:

σ_r = true stress

The true stress also can be written by the Equation 6:

$$\sigma_r = k\varepsilon^{-n} \tag{6}$$

Where:

k = strength coefficient.

ε = total plastic strain.

n = strain-hardening.

Forming Limit Diagram.

The samples to obtain the forming limit diagram (FLD) were initially cut in squares (180x180) mm and then, using a digital height gage, a quadratic mesh (5x5) mm was created in one side of each sample. The samples were subdivided in 6 others parts, as in Figure 4.

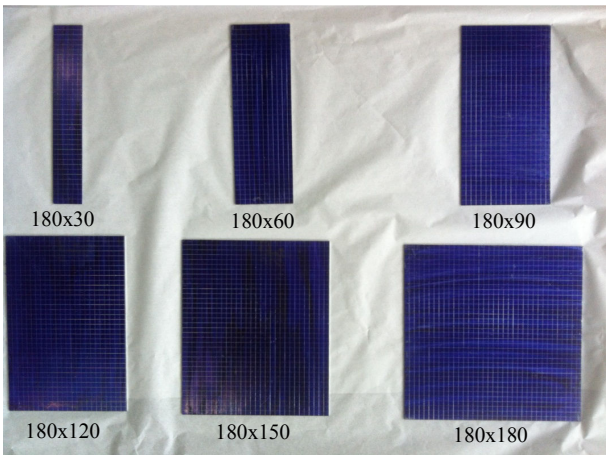

Figure 4 – Samples to obtain the FLD, dimensions in millimeters.

The tests to obtain the FLD were done using hydraulic press of simple effect with a nominal capacity of 100 kN. The sheet samples were placed on the inferior base of the stamping die, then the stamping die was closed using 80 kN as press plates. The increase in load was done constantly with velocity of 3,4 mm/s until the cracking of sheets. The Nakazima test method was used for determination of FLDs, this method uses a hemispherical punch as the Figure 5.

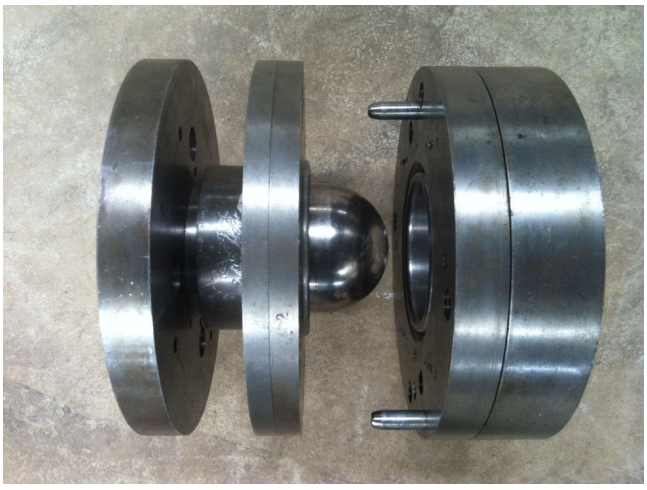

Figure 5 – Nakazima hemispherical punch.

The deformation measurements were taken in the fracture area and proximities. The rectangles were classified in three differents types for a correct interpretation of results:

Type 1 – Fracture, there is a fracture through the rectangle;

Type 2 – Affected by the fracture (necking), the rectangle is near of the area affected by the fracture.

Type 3 – Sane area, the rectangle isn't in the area affected by the fracture.

The rectangle type 1 was measured in the largest dimension minus the width of the fracture, in order to provide the parameter ε_1. The parameter ε_2 was taken in the smallest width. The rectangle type 2 was measured near the fracture, in a necking area. The rectangle type 3 was measured far from fracture.

The major strain (E1) and the minor strain (E2) were calculated using the equations 7 and 9, respectively.

$$E_1 = \ln(1 + \varepsilon_1) \tag{7}$$

$$\varepsilon_1 = \frac{D_{f1} - D_{i1}}{D_{i1}} \tag{8}$$

$$E_2 = \ln(1 + \varepsilon_2) \tag{9}$$

$$\varepsilon_2 = \frac{D_{f2} - D_{i2}}{D_{i2}} \tag{10}$$

Where:

D_{f1}=Major strain measured;

D_{f2}=Minor strain measured;

D_{i1}=D_{i2}= Initial measure;

ε_1= ε_2=Conventional strain;

E_1= E_2=True strain;

RESULTS AND DISCUSSION

Chemical Analysis

The table 1 shows the chemical composition required for steel FE E340, being also possible see the values found for this material.

Table 1- Chemical composition of steel FE E340.

CHEMICAL COMPOSITION [%]									
STEEL		**C max.**	**Mn max.**	**P max**	**S max.**	**Al min.**	**Si max.**	**Nb**	**Nb+Ti+V max.**
SPECIFIED	FE E340	0,12	1,5	0,03	0,03	0,015	0,5	0,15÷0,40	0,2
FOUND		0,0860	0,5420	0,0134	0,0080	0,0350	0,0100	0,0271	0,0387

The table 2 shows the chemical composition required for steels FE 600DP and FE 800DP, being also possible to see the values found for these materials.

Table 2 - Chemical composition of steels FE 600DP and FE 800DP.

CHEMICAL COMPOSITION [%]									
STEEL		**C max.**	**Mn max.**	**Al min.**	**Si max.**	**P max**	**S max.**	**Cu max.**	**B max.**
SPECIFIED	DP	0,23	3,3	0,01	2,5	0,09	0,015	0,2	0,006
FOUND	FE 600DP	0,1170	1,8240	0,0514	0,2280	0,0227	0,0064	0,0090	0,0000
FOUND	FE 800DP	0,1370	1,7180	0,0380	0,2400	0,0230	0,0083	0,0300	0,0000

The chemical analysis results found for each material shows that these materials are in accordance with their established specifications.

The chemical composition of steel FE E340 has micro-alloying elements as Niobium (Nb), Titanium, and Vanadium. These elements have two important characteristics; increase in its mechanical strength and increase in its forming ability.

Metallographic Analysis

The figure 6 shows the material FE E340 microstructure increased by 100x, being possible see a refined structure and grain size 10 as ASTM E-112.

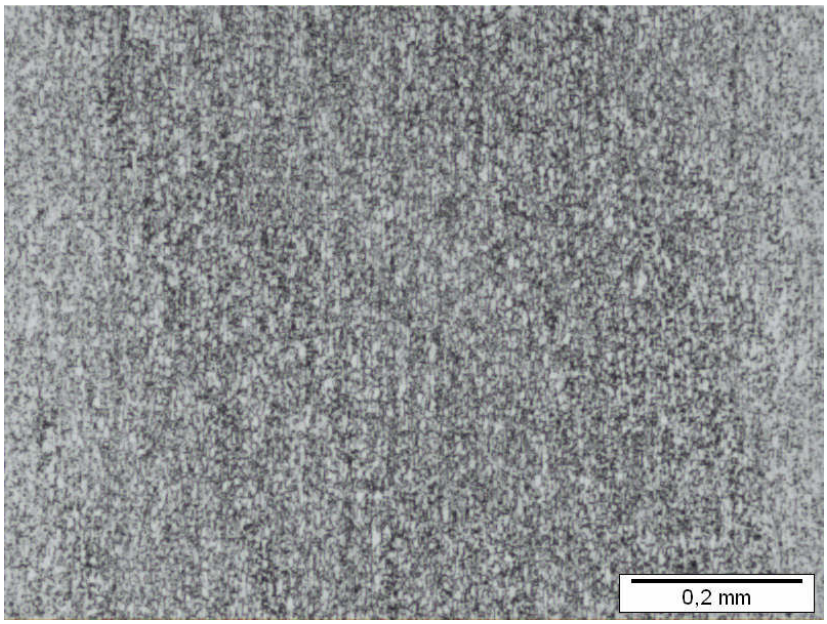

Figure 6 – FE E340 microstructure, attack Nital 10%; increase 100x.

The figure 7 shows the material FE E340 microstructure increased by 500x, the microstructure is composed basically of fine-grained ferrite uniformly distributed.

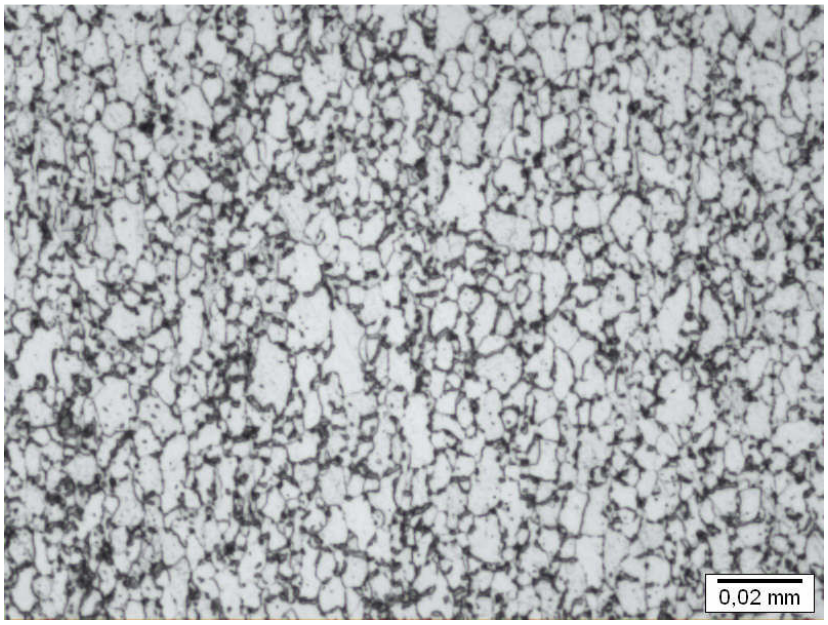

Figure 7 - FE E340 microstructure, attack Nital 10%; increase 500x.

The figure 8 shows the material FE 600DP microstructure increased by 500x, the microstructure is a ferrite matrix and martensite as a second phase.

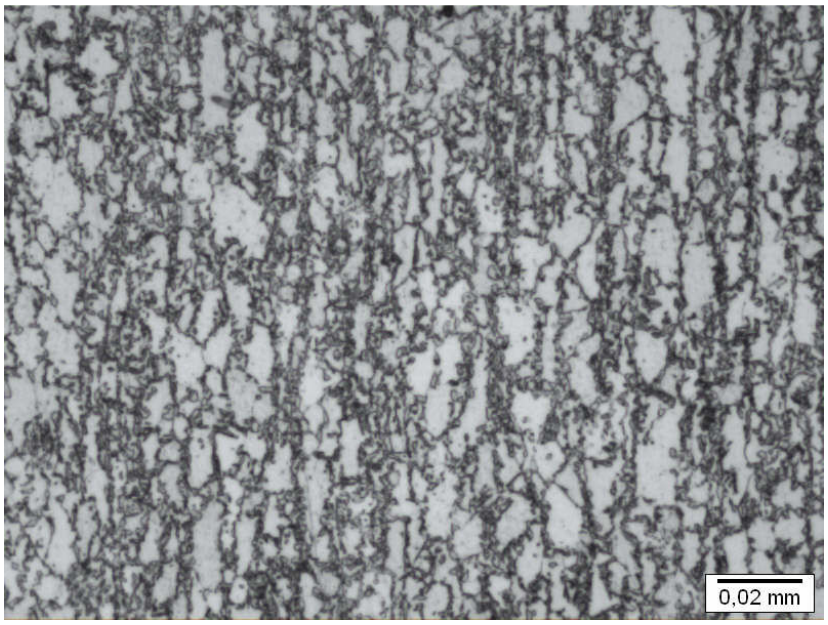

Figure 8 - FE 600DP microstructure, attack Nital 10%; increase 500x

The figure 9 shows the material FE 800DP microstructure increased by 500x, the microstructure is a ferrite matrix and martensite as a second phase. In this micrograph there is a greater density of martensitic phase compared as micrograph of material FE 600DP.

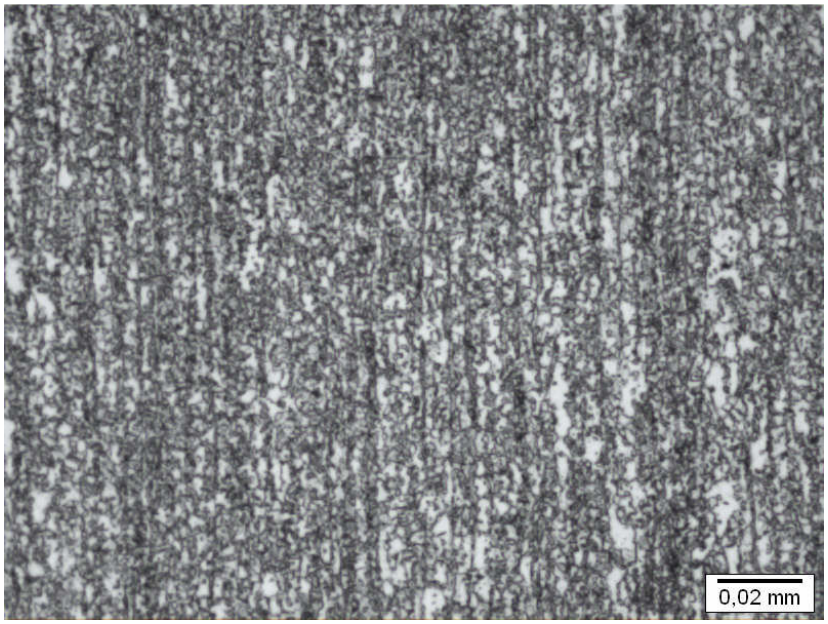

Figure 9 - FE 800DP microstructure, attack Nital 10%; increase 500x

Microhardness Testing

The global average hardness of materials was:

- FE E340 - 178HV/10;
- FE 600DP - 195HV/10;
- FE 800DP - 234HV/10;

Tensile Testing

The table 3 shows the average results obtained in the tensile tests for all three materials.

Table 3 – Mechanical characteristics of materials FE E340, FE 600DP and FE 800DP

MECHANICAL CHARACTERISTICS							
STEEL		FE E340		FE 600DP		FE 800DP	
		TRANS	LONG	TRANS	LONG	TRANS	LONG
FOUND	Yield Strength [MPa]	394	386	369	371	460	427
	Ultimate tensile strength [MPa]	489	490	650	654	811	792
	Elongation [%]	28	25	20	26	17	19
	Strain-hardening [n]	0,11	0,14	0,18	0,19	0,14	0,13
SPECIFIED	Yield Strength [MPa]	340÷420		340÷440		420÷550	
	Ultimate tensile strength [MPa]	410		590		780	
	Elongation – minimum [%]	23		20		15	
	Strain-hardening – minimum [n]	0,13		0,14		0,11	

The figure 10 shows the curve of tensile testing for three materials tested. The main difference between the materials is the ultimate tensile strength.

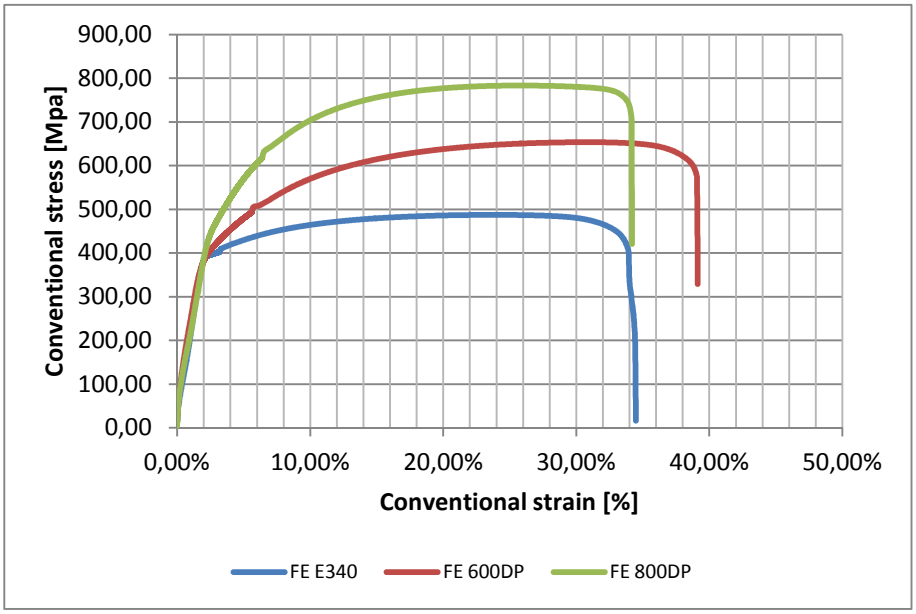

Figure 10 – Conventional strain-stress curve.

The figure 11 shows the true strain-stress curve for materials studied.

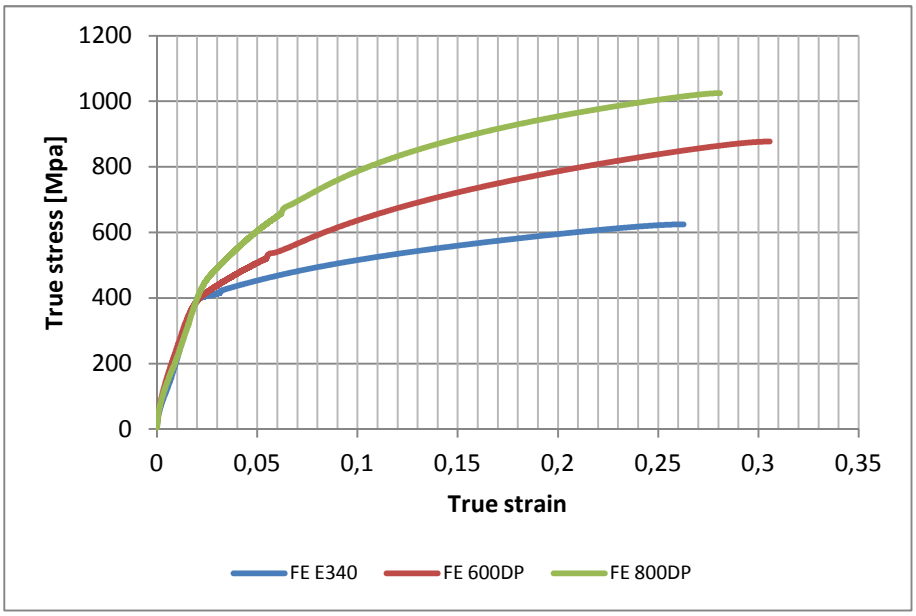

Figure 11 – True strain-stress curve.

The results presented in table 3 shows that measured values are in accordance with their specifications and they confirm their good characteristics of formability and high strength.

The strain-hardening (n) of material FE 600DP was grater compared to the other two materials studied, as this feature indicates better formability than others, especially in necking operations. The curves of tensile tests show that the materials have an yield strength very close to each other, and that the ability of the materials to deform plastically fit at the same level. The major differences for the three materials are around the ultimate tensile strength and elongation of each one.

Forming limit diagram.

The figure 12 shows the forming limit diagrama (FLD) for FE E340 material. The diagram was plotted with two main curves, the lower curve was plotted based in the measure taken in rectangle type 3 and the upper curve was plotted based in the measure taken in recangle type 1.

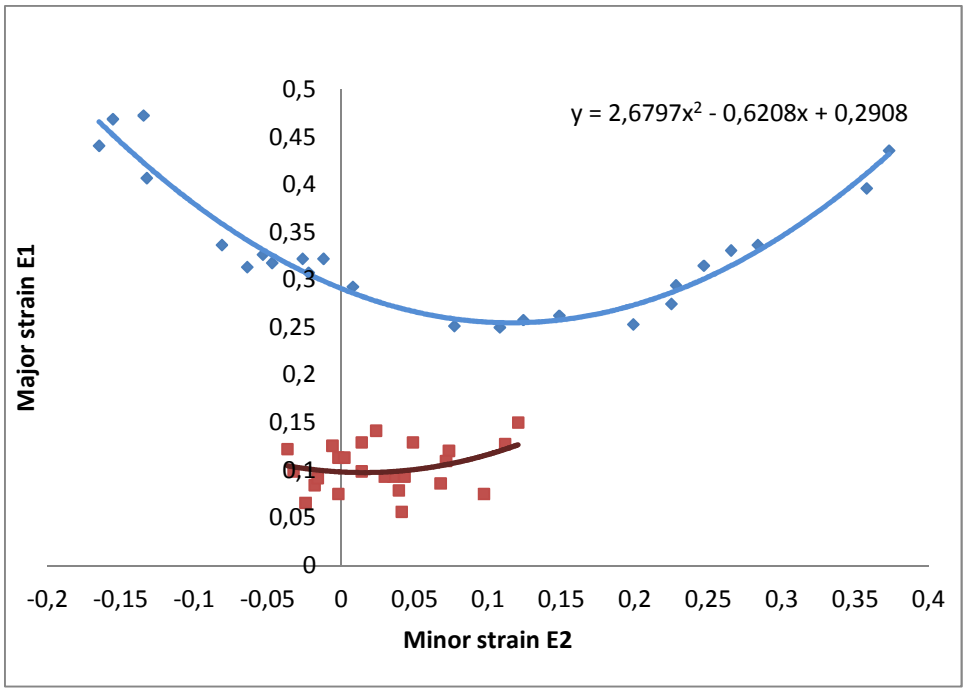

Figure 12 – Forming limit diagram, material FE E340.

The figure 13 shows the forming limit diagrama (FLD) for FE 600DP material. This material has the higher strain-hardening (n) among the materials studied. The higher strain-hardening means better deformation absortion ability without necking.

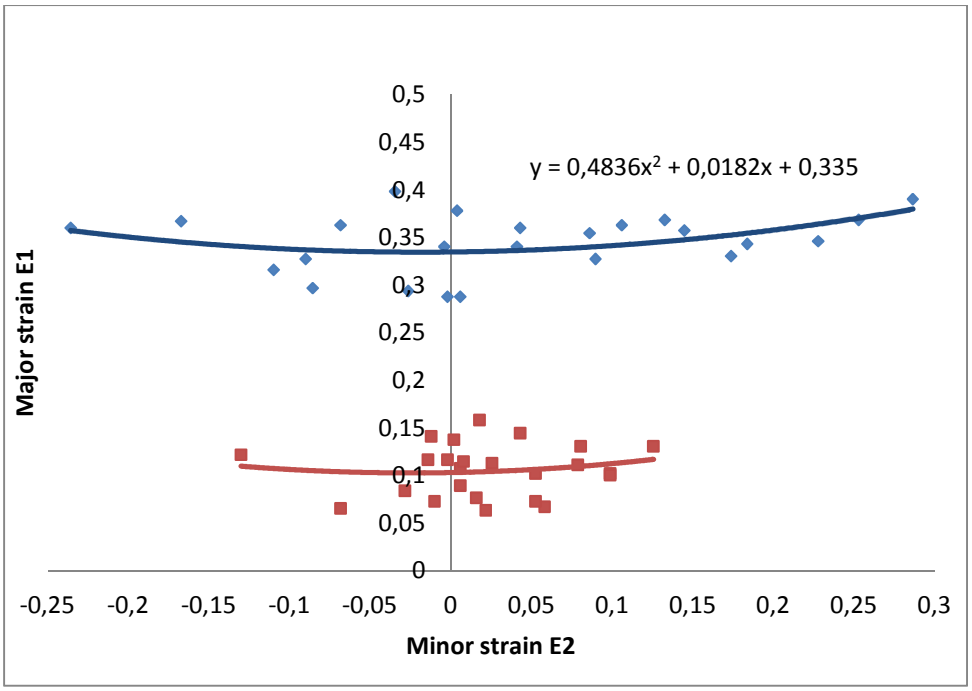

Figure 13 – Forming limit diagram, material FE 600DP.

Figure 14 shows the deformation limit diagram (FLD) for the material 800DP FE. This material has lower capacity for deformation absorption among the materials studied. It is important to take into account the thickness of the material and its high density of martensite. The small thickness reduces the ability of the material to deform without stretching or fracture. The high density of martensite is responsible for making the material fragile and brittle.

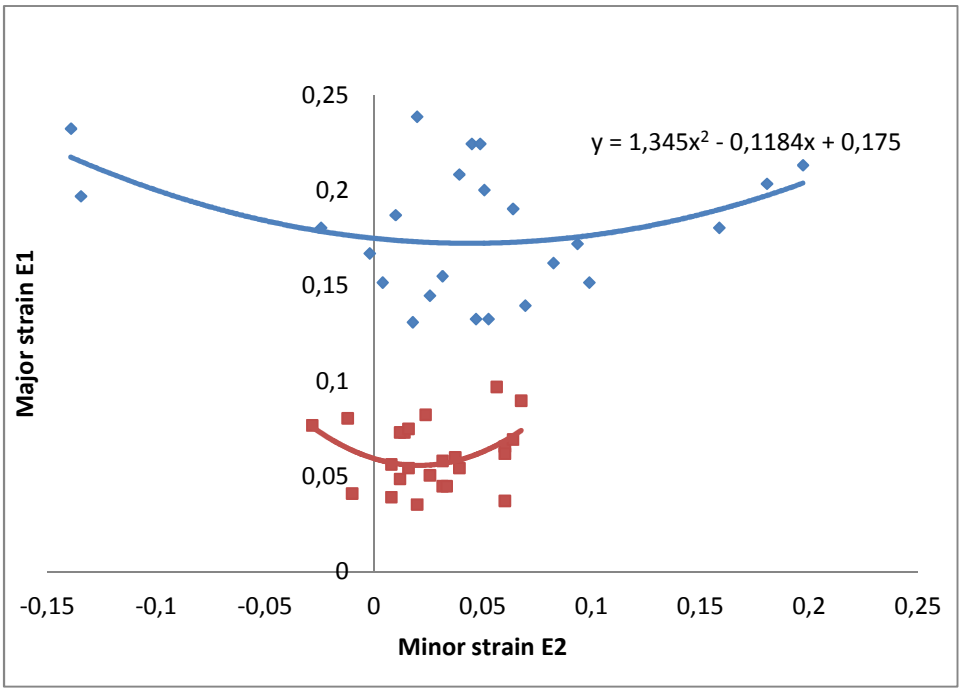

Figure 14 – Forming limit diagram, material FE 800DP.

The figure 15 shows a comparison between materials FE E340 and FE 600DP. The material FE E340 has high capacity to absorb compressive strains, while the material FE 600 DP has a FLD more uniform and better able to absorb tensile strains.

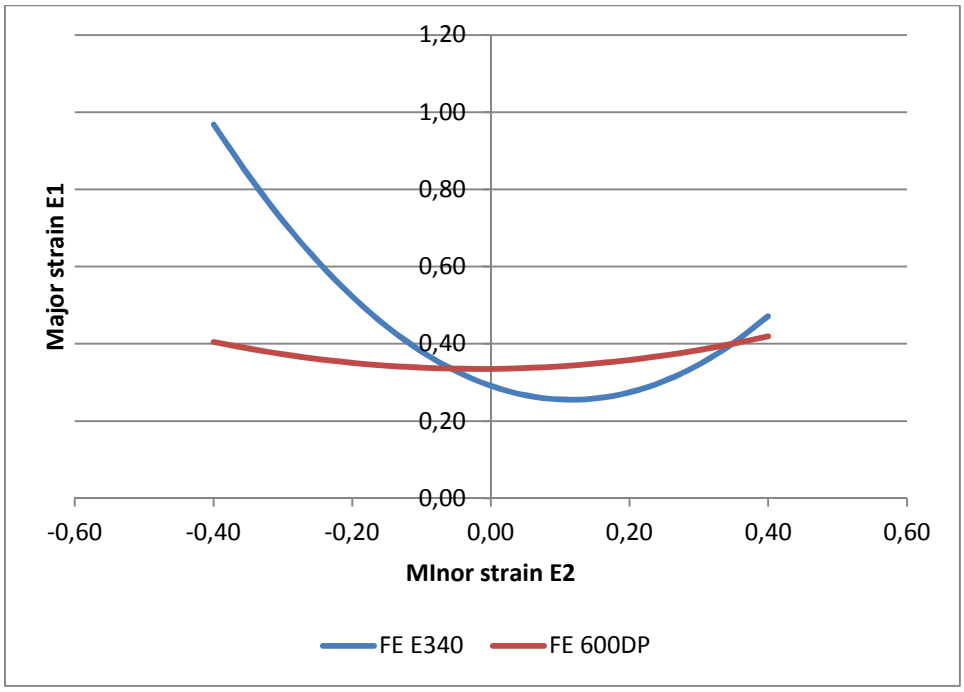

Figure 15 – Comparison between FE E340 and FE 600DP.

The figure 16 shows a comparison between materials FE 600DP and FE 800DP. The material FE 800DP has low capacity to absorb deformations without fracture.

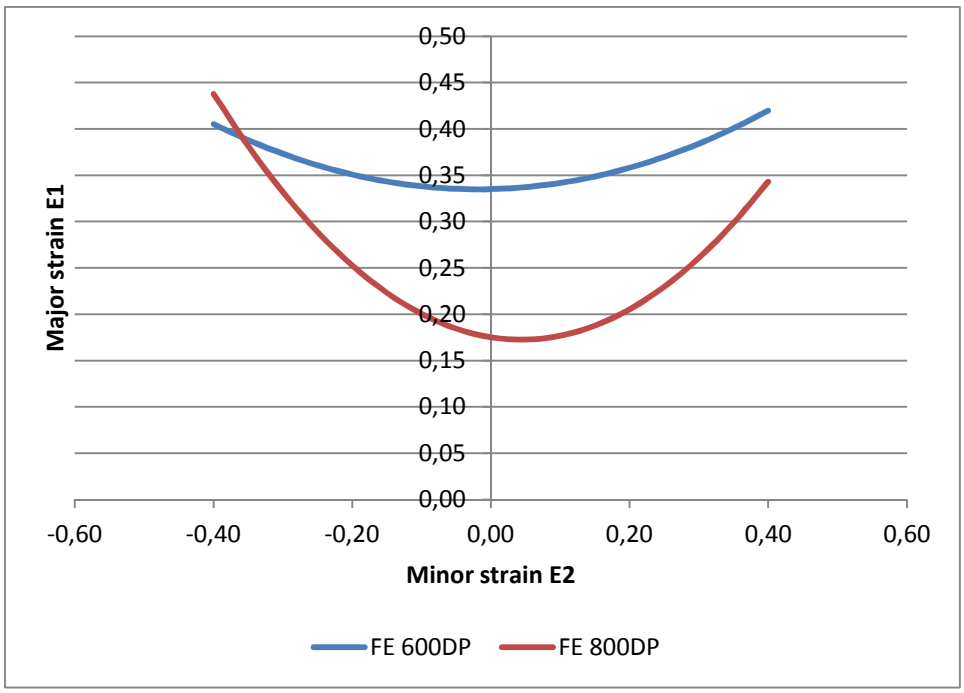

Figure 16 - Comparative between FE 600DP and FE 800DP.

The figure 17 shows the samples, used to build a FLD, after a forming process.

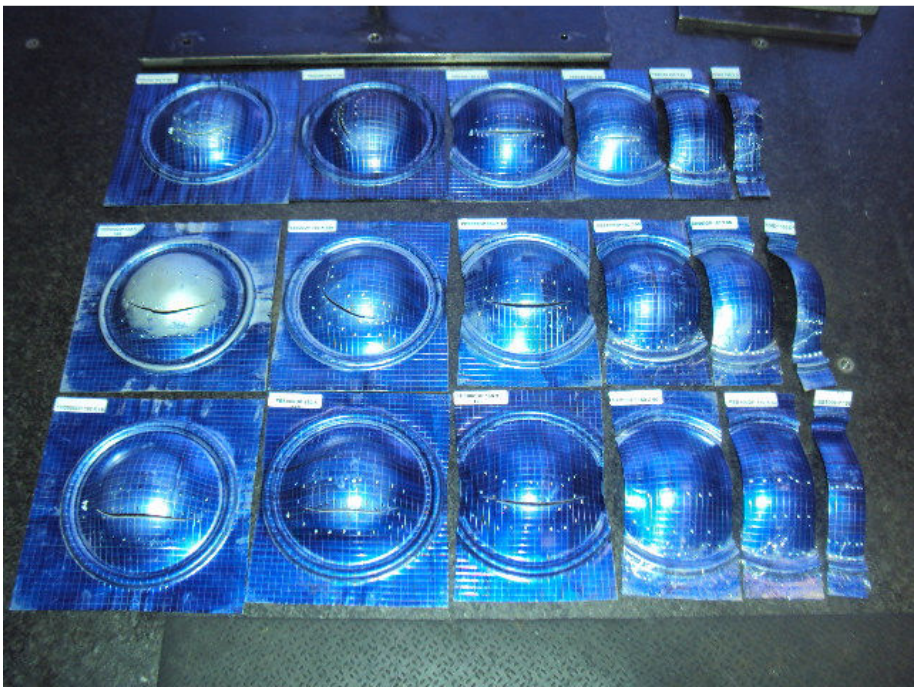

Figure 17 – Samples used in forming limit diagram test.

CONCLUSION

- The microstructure of the steel FE E340 is typically High Strength Low Alloy steel (HSLA) developed for stamping of components relatively complex.
- The microstructures of steels FE 600DP and FE 800DP are typical of an Advanced High-Strength Steel (AHSS). If the fraction of martensite is varied, it is also possible to vary their mechanical strength.
- The selection of a material should not only take into account cost and mechanical strength. The forming limit diagram (FLD) was important to determine the stampability of each material and then it is possible to optimize the process and reduce waste.
- Taking into account the characteristics required for the B-pillar reinforcement as: high strength, lightweight, and good stampability, the material FE 600DP is the most recommended because it is able to combine all of these features.

ACKNOWLEDGMENTS

The authors gratefully acknowledge FIAT Automóveis S.A and Brasiaço Industría e Comércio for the resources made available for the completion of this project.

REFERENCES

ALMEIDA, Tarcisio José. **Estudo da Conformabilidade de Chapas de Aço Livre de Intersticiais em Prensas Hidráulicas de Simples Efeito.** 1998. Tese (Mestrado em Engenharia) – Escola de engenharia da UFMG. Belo Horizonte, Minas Gerais.

BLECK, Wolfgang; DENG Zhi; PAPAMANTELLOS, Kostas; GUSEK, Christopher Oliver. **A comparative study of the forming-limit diagram models for sheet steels**. Journal of Materials Processing Technology. 1997. p 223-230.

CORA, Ömer Necati; KOÇ Muammer. **Experimental investigations on wear resitance characteristics of alternative die materials for stamping of advanced high-strength steels (AHSS)**. International Journal of Machine Tools & Manufacture. 2009. p 897-905.

HILL, Robert e Reed. **Physical Metallurgy Principles**. 2ª edição. Londres: D. Van Nostrand Company,1973.

KUZIAK, R.,KAWALLA, R., WAENGLER S. **Advanced high strength steels for automotive industry.** Arquives of civil and mechanical engineering. 2008. p 105-117.

LORA, Fábio André. **Avaliação do processo de estampagem profunda de chapas de aço BH 180 e BH 220 utilizado na indústria automobilística**. 2009. Tese (Mestrado em engenharia) – Universidade Federal do Rio Grande do Sul, Porto Alegre.

ULSAB-AVC. **Technical Transfer Dispatch #6**: ULSAB-AVC Body Structure Materials. ULSAB-AVC Consortium. 2001. p 9.

WORLD AUTOSTEEL. **Advanced high strength steel (AHSS) application guidelines.** 2009. p 163

WU-RONG, Wang; CHANG-WEI, He; ZHONG-HUA, Zhao; XI-CHENG, Wei. **The limit drawing ratio and formability prediction of advanced high strength dual-phase steels**. Materials and Design. 2011. p 3320-3327.